Non-Isothermal Flow of CO_2 in Injection Wells: Evaluation of Different Injection Modes

Orlando Silva
Amphos 21 Consulting S.L.
Passeig Garcia i Faria, 49-51, 08019, Barcelona, Spain, orlando.silva@amphos21.com

Abstract: Injection conditions of CO_2 at the wellhead may play a major role on the flow behavior through the wellbore. The density and the injection rate reached at the bottomhole are key factors affecting the performance and efficiency of CO_2 geological storage. In this work a model of non-isothermal flow of CO_2 in injection wells is developed in Comsol and used to assess different injection strategies.

Keywords: CO_2 sequestration, transient wellbore flow, thermodynamics; energy resources.

1. Introduction

During the injection of carbon dioxide (CO_2), the fluid density within the injection pipe could vary significantly along the well in response to pressure and temperature variations, thus affecting the CO_2 injection rate at the reservoir depth (Figure 1). Among other reasons, understanding the behavior of CO_2 flow through injection and monitoring wells is crucial because: (i) CO_2 flow through the injection wells is the linking step between transport and storage (Nimtz *et al*., 2010; Pan and Oldenburg, 2014); (ii) the adopted injection strategy may affect significantly the energy consumption and efficiency of CO_2 geological storage (Vilarrasa *et al*., 2013); (iii) design and control of the operation both at pilot and industrial scale.

Flow of CO_2 in non-isothermal wells involves solving the partial differential equations (PDE) that express energy, mass and momentum conservation. These PDEs are coupled through equations of state (EOS) governing fluid and thermodynamic properties (Lu and Connell, 2008; Han *et al*., 2010; Pan *et al*., 2011; Sponagle *et al*., 2011).

In the present work, a one-dimensional (1D) model for non-isothermal single-phase flow of CO_2 through injection wells is developed in Comsol Multiphysics and applied to evaluate different injection modes and hypothetical CO_2 injection scenarios.

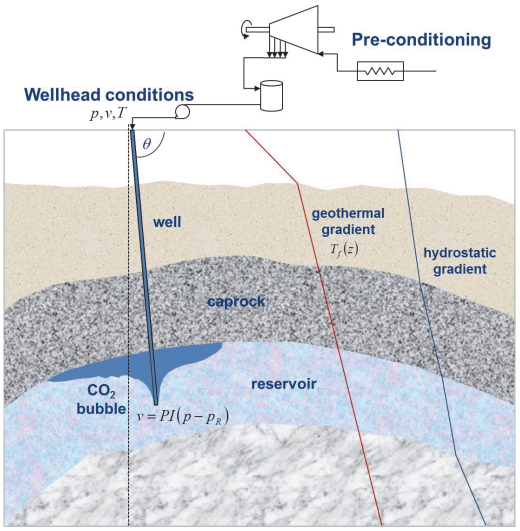

Figure 1. CO_2 injection through a wellbore.

2. Methodology

The methodology used to implement in Comsol the present 1D non-isothermal single-phase flow of CO_2 in injection wells, follows the approach of Lu and Connell (2014), in which the flow equations are based on the averaged-flow model (Hasan and Kabir, 2002).

2.1 Governing Equations

Flow of CO_2, or any fluid, and its mixtures in non-isothermal wells involves solving the PDE that express energy, mass and momentum conservation. The governing equations are derived from a general form for two-phase flow, here applied to the specific case of single-phase flow (e.g., pure gas or liquid). With the transient terms included, the governing equations describing non-isothermal one-dimensional flow in wells can be expressed as follows:

$$\frac{\partial \rho}{\partial t} + \rho \frac{\partial v}{\partial z} + v \frac{\partial \rho}{\partial z} = 0 \qquad (1)$$

$$\frac{\partial v}{\partial t} + v \frac{\partial v}{\partial z} + \frac{1}{\rho} \frac{\partial p}{\partial z} = -f_\mu \frac{v^2}{2d} + g \sin\theta \qquad (2)$$

$$\frac{\partial h}{\partial t}+v\frac{\partial h}{\partial z}-\frac{1}{\rho}\frac{\partial p}{\partial t}+v\frac{\partial v}{\partial t}+v^2\frac{\partial v}{\partial z}= \\ -vg\sin\theta-\frac{\pi d q(z,t)}{\rho A} \tag{3}$$

In equations (1-3), t is time and z denotes the one-dimensional coordinate along the length of the wellbore. Length is used instead of depth in terms of the z-coordinate, because the injection tubing may include horizontal or inclined sections. v is the average velocity, p is the pressure, h is the specific enthalpy of CO_2, g is the gravity, θ is the inclination angle of the wellbore, d is the internal diameter of the injection tubing, A is the cross section area ($A=\pi d^2/4$), f_μ denotes the Moody friction factor and q is the heat exchange flux between the fluid and its surroundings (wellbore and formation), which here is described by $q(z)=-\pi d U_\infty\left(T-T_f(z)\right)$, where U_∞ is the overall-heat-transfer coefficient for wellbores, T is the CO_2 temperature and $T_f(z)$ describes the distribution of the formation temperature along the injection well. On the other hand, h is expressed as a function of p and T using thermodynamics (Lu and Connell, 2014)

$$dh=C_p\left(dT-\eta dP\right) \tag{4}$$

where C_p is the specific heat of CO_2 at constant pressure, and $\eta=T\left(\left(\partial\hat{V}/\partial T\right)_p-\hat{V}\right)$ is the Joule-Thompson coefficient ($\hat{V}$ denotes the molar volume of CO_2). Eq. (4) is used to express Eq. (3) in terms of T as state variable instead of h.

2.2 Boundary and initial conditions

Two typical operating conditions at the wellhead are flowrate-controlled and pressure-controlled injection, respectively. For flowrate-controlled injection, a Dirichlet boundary condition is set at the inlet specifying p, T and v, while at the bottomhole no boundary is considered. For pressure-controlled injection a boundary condition relating the flowrate and the reservoir pressure at the bottom of the well can be specified as

$$v=PI\left(p-p_R\right)A \qquad z=L \tag{5}$$

where L is the well length, PI stands for the local well productivity index and p_R is the local reservoir pressure.

It is assumed that the CO_2 is initially static in the well at a uniform injection temperature and a pressure distribution given by hydrostatic and the pressure injection at the wellhead.

2.3 Constitutive relationships

As far as fluid properties are concerned, density and heat capacity of CO_2 were calculated according to the Redlich-Kwong EOS (Redlich and Kwong, 1949) using the parameters proposed by Spycher *et al*. (2003). Viscosity was calculated according to the correlation of Altunin and Sakhabetdinov (1972). The friction factor was computed considering both laminar and turbulent flow. The last was calculated according to the Zigrang and Sylvester (1985) correlation, assuming a rugosity of the injection pipe equal to 0.36 mm.

2.4 Implementation in Comsol

The model equations were implemented in Comsol through the coefficient's form of the PDE module with multiple dependent variables

$$\mathbf{e_a}\frac{\partial^2\mathbf{u}}{\partial t^2}+\mathbf{d_a}\frac{\partial\mathbf{u}}{\partial t} \\ -\nabla\cdot\left(\mathbf{c}\nabla\mathbf{u}+\boldsymbol{\alpha}\mathbf{u}-\boldsymbol{\gamma}\right)+\boldsymbol{\beta}\cdot\nabla\mathbf{u}+\mathbf{a}\mathbf{u}=\mathbf{f} \tag{6}$$

where $\mathbf{u}=\left(p,v,T\right)^T$, $\mathbf{e_a}=\mathbf{c}=\boldsymbol{\alpha}=\mathbf{0}$, $\boldsymbol{\gamma}=\mathbf{0}$ and

$$\mathbf{d_a}=\begin{pmatrix}\partial\rho/\partial p & 0 & 0\\ 0 & 1 & 0\\ -\left(1/\rho+\eta\right) & v & C_p\end{pmatrix} \tag{7a}$$

$$\boldsymbol{\beta}=\begin{pmatrix}v\,\partial\rho/\partial p & \rho & 0\\ 1/\rho & v & 0\\ -v\eta & v^2 & vC_p\end{pmatrix} \tag{7b}$$

$$\mathbf{a}=\begin{pmatrix}0 & 0 & 0\\ 0 & -f_\mu v/2d & 0\\ 0 & -g\sin\theta & 4U_\infty/\rho d\end{pmatrix} \tag{7c}$$

$$\mathbf{f} = \begin{pmatrix} 0 \\ -g\sin\theta \\ 4U_\infty T_f(z)/\rho d \end{pmatrix} \quad (7d)$$

All constitutive relationships were implemented as local equations by using Comsol variables. The domain was discretized considering a uniform mesh of 1000 elements. Stationary and time-dependent studies were defined to solve the problem in steady state and transient. In both cases the system of equations (6) was solved with a fully coupled Newton-Raphson iteration scheme.

3. Injection modes

Seven simulations were run to study different CO_2 injection conditions at the wellhead: gas, gas and liquid near the critical point (CP), supercritical (SC) (8 and 10 MPa), liquid at high p and T, liquid at low p and T (Table 1 and Figure 2). The energy consumption due to surface conditioning operations varies for each injection mode and can be roughly estimated by the difference of specific enthalpy between wellhead and storage vessel conditions (Vilarrasa *et al.*, 2013). Table 1 shows the energy consumption for each injection mode (storage vessel at 2.0 MPa and -20 ºC; injection flowrate of 1.0 kg/s). It is higher when injecting CO_2 in gas-phase, near critical and SC conditions at the wellhead. On the contrary, injecting CO_2 in liquid-phase reduces substantially the energy consumption because pumping/compression is easier and heating is minor.

Table 1: CO_2 injection modes simulated in this work

	Injection conditions	p, MPa	T, ºC	Compression work, kW
1	Gas	4.5	35	305.7
2	Gas near CP	7.0	31	245.4
3	Liquid near CP	8.0	31	125.8
4	Supercritical	8.0	40	241.3
5	Supercritical	10.0	40	146.6
6	Liquid	8.0	25	103.11
7	Liquid	5.0	-10	19.66

CP: critical point

In all the simulations, the surface temperature is assumed to be -5 ºC (winter conditions) with a geothermal gradient being 0.12 ºC/m for the depth of the first 200 m and then 0.033 ºC/m for the following. The internal diameter of the injection pipe was set at 10 cm and the wellbore is assumed to be vertical (θ = 90º). The bottom of the injection pipe is located at 1000 m, coinciding with the top of a hypothetical aquifer for CO_2 storage. In addition, a mass flow rate of 1.0 kg/s and an overall heat transfer coefficient of U_∞ = 4 W m^{-2} K^{-1} were considered in the simulations.

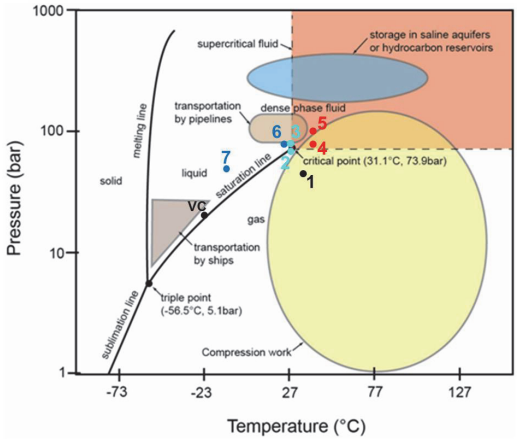

Figure 2. CO_2 phase diagram: pipeline transportation is done in liquid conditions and geological storage stays in supercritical conditions. Color dots and numbers represent 7 injection conditions at the top of the well (Table 1) (VC stands for vessel conditions).

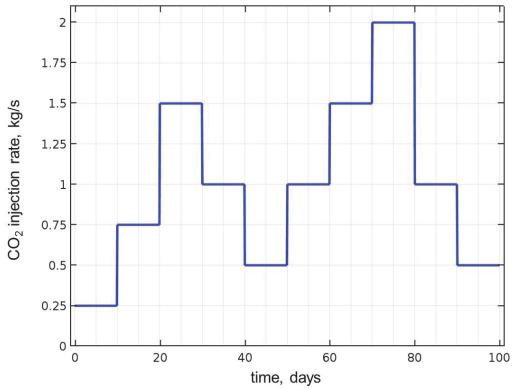

Figure 3. Fluctuating CO_2 injection regime.

Two additional simulations were run to study the effect of injecting SC CO_2 at 8.0 MPa and 40 ºC (Table 1): (i) with variable flowrate and (ii) under pressure-controlled injection. In (i) a fluctuating injection regime is defined by a piecewise function in Comsol (Figure 3), such that the total mass of injected CO_2 during 100

days is equal to the mass injected at a constant rate of 1.0 kg/s in the same period (8640 ton of CO_2). In (ii), the well productivity index is set at 6×10^{-7} m s^{-1} N^{-1} and the reservoir pressure in the near-field of the well is assumed to increase in time due to CO_2 injection according to the evolution depicted in Figure 4. This p_R increase was defined in Comsol by using a piecewise cubic interpolation function.

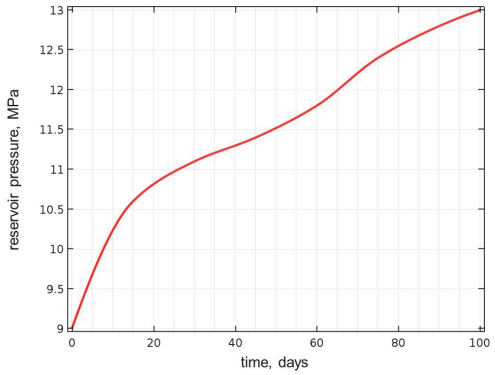

Figure 4. p_R increase due to CO_2 injection assumed to simulate pressure-controlled injection.

4. Results and Discussion

4.1 Different wellhead conditions

Figure 5 shows the temperature, pressure, velocity and density profiles obtained in steady state for each injection mode. Injecting gaseous CO_2 causes very low densities through the wellbore. CO_2 injection in gaseous near the CP and SC (8 MPa) conditions increase density but at the bottom this is still lower than 600 kg/m^3. By contrast, injecting liquid near the CP and SC (10 MPa) conditions lead to higher bottomhole densities, comparable to those reached by injecting liquid CO_2. Higher CO_2 densities are advantageous because are closer to the density of the resident brine, which reduce buoyancy effects in the reservoir and the potential risks of caprock failure and subsequent CO_2 leakages.

Secondly, transient simulations reveal that steady state is reached faster by injecting at higher pressures. In particular, steady state flow conditions are obtained after 1 hour when injecting SC CO_2 at the wellhead (Figure 6). On the contrary, operational equilibrium is reached only after 100 days by injecting gaseous or liquid CO_2 at low pressure (Figure 7).

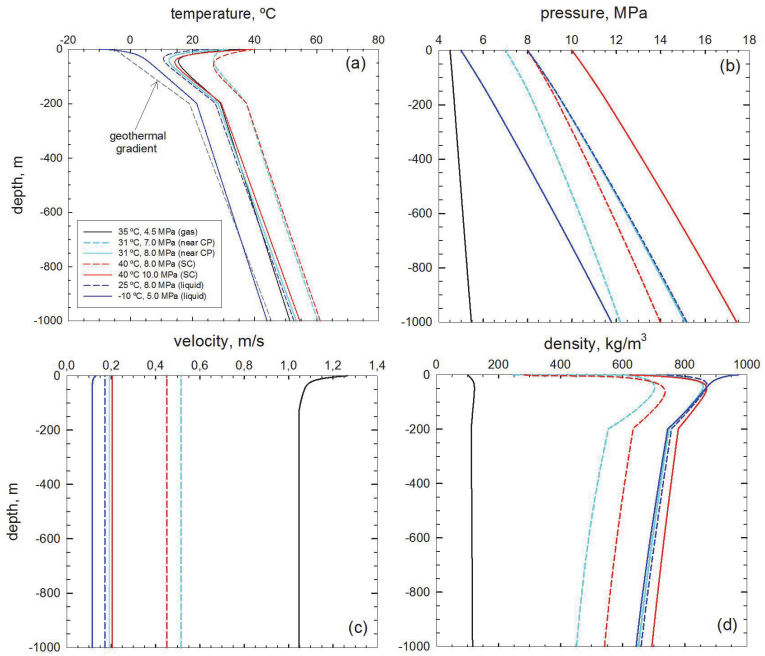

Figure 5. Comparison of different injection modes (Table 1): temperature (a), pressure (b), velocity (c), and density (d) profiles in steady state.

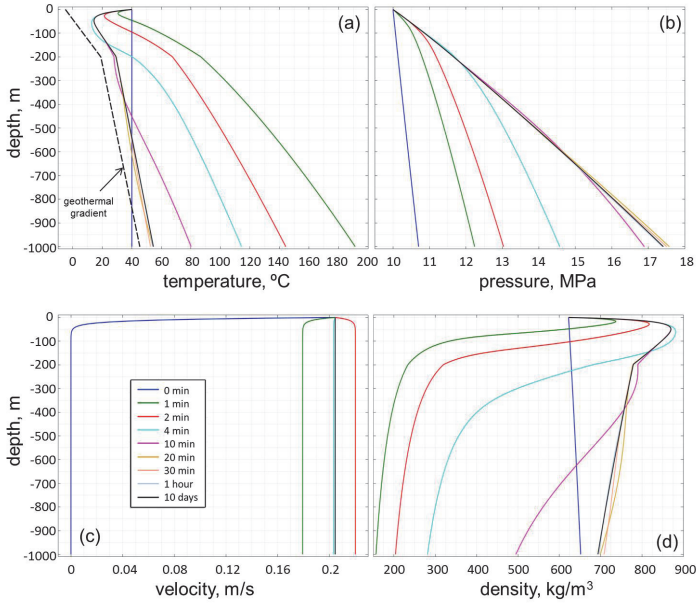

Figure 6. Evolution of temperature (a), pressure (b), velocity (c), and density (d) profiles. CO_2 is injected SC (40 ºC and 10 MPa) at 1.0 kg/s. Steady state is reached after 1 hour.

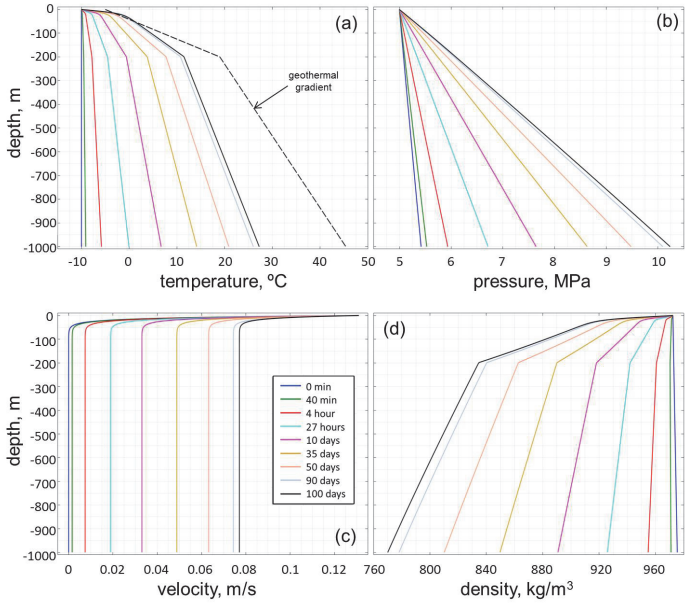

Figure 7. Evolution of temperature (a), pressure (b), velocity (c), and density (d) profiles. CO_2 is injected liquid (-10 ºC and 5 MPa) at 1.0 kg/s. Steady state is reached after 100 days.

4.2 Fluctuating CO_2 injection

Injecting CO_2 at variable flowrate can help to increase considerably the density of CO_2 at the bottomhole. Figure 8 shows that an average density increase of about 18% is obtained at the bottomhole (compare Figure 8b and d), despite there are periods in which CO_2 heating due to the friction within the injection pipe can induce a notorious density reduction (Figure 8c and d). Nevertheless, it has been demonstrated that a fluctuating injection regime can enhance CO_2 dissolution into the resident brine of the storage

aquifer (Hidalgo and Carrera, 2009). Therefore, the present simulation shows that this injection mode has the double advantage of reducing the pressure within the reservoir and improving the efficiency of CO_2 storage.

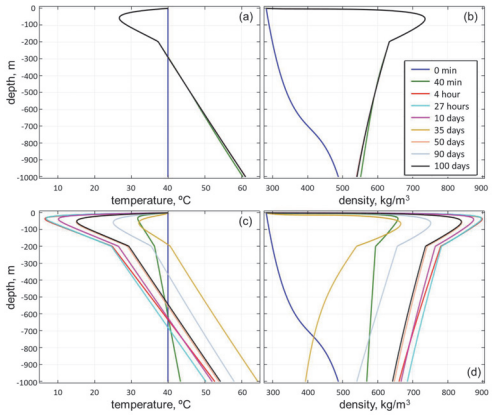

Figure 8. Temperature and density evolution under constant (a, b) and fluctuating (c, d) injection regime.

4.3 Pressure-controlled injection

Pressure-controlled injection may be more realistic operating conditions. Even more, it provides a way for coupling models for CO_2 flow through the well and multiphase flow and transport of CO_2 through the geological formations (reservoir and caprock). Nevertheless, pressure-controlled injection causes variable mass injection flowrates, which can reduce substantially the efficiency of storage. A comparison between the steady state p, v, T and ρ profiles obtained under flowrate-controlled injection and pressure-controlled injection with a constant reservoir pressure of 10 MPa is presented in Figure 9. Due to the lower heating (Figure 9a) and the higher pressures (Figure 9b) developed through the injection string, the CO_2 density increases significantly under pressure-controlled injection (Figure 9d). However, the higher density is compensated by a reduction of the injected mass of CO_2. The velocities decrease in more than one order of magnitude (Figure 9c), which results in a total injected mass of CO_2 of about 1322 ton in 100 days.

The situation is even worse when considering the effect of a dynamic reservoir pressure. The increase of the reservoir pressure due to the evolution of a CO_2–rich phase within the storage formation reduces the injection rate (Eq. 5).

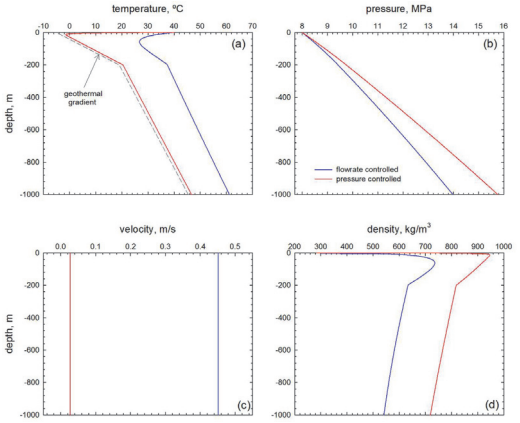

Figure 9. Flowrate-controlled versus pressure-controlled (p_R = 10 MPa) injection: temperature (a), pressure (b), velocity (c), and density (d) profiles in steady state. CO_2 is injected SC at 40 ºC and 8 MPa.

For the assumed p_R increase (Figure 4), the total mass of CO_2 injected in 100 days is now about 980 ton. In contrast, the CO_2 densities through the injection well are substantially increased (Figure 10d), as a consequence of the stronger cooling of the well (Figure 10a). This is due to the lower velocities (Figure 10c) that allow CO_2 to exchange heat with the surrounding for longer times. In fact, the CO_2 temperature approaches the geothermal gradient quickly, such that after 10 days there is a temperature difference of only 1 ºC between them in most of the wellbore (Figure 10a).

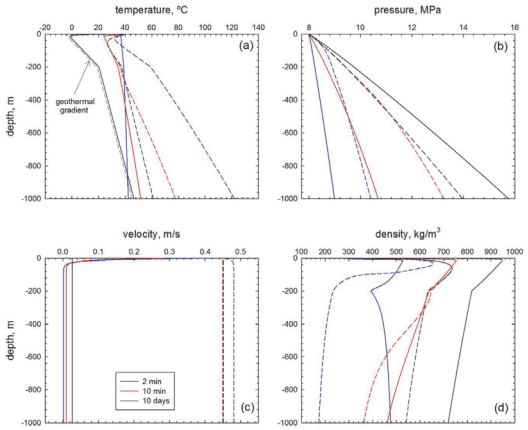

Figure 10. Flowrate-controlled (dashed line) versus pressure-controlled injection with variable p_R (solid line). Evolution of temperature (a), pressure (b), velocity (c), and density (d) profiles. CO_2 is injected SC at 40 ºC and 8 MPa.

5. Conclusions

A 1D model for non-isothermal single-phase flow of CO_2 through injection wells has been implemented in Comsol. This implementation can be used for the assessment of several injection modes. In particular, the simulations performed in this work allowed to compare different operating conditions at the wellhead, which can represent hypothetical scenarios of CO_2 pre-conditioning at surface.

The results show that wellhead conditions of CO_2 below the critical point cause low fluid densities through the injection pipe. Conversely, injecting liquid CO_2 or CO_2 at high pressure helps to increase the density at the bottomhole, which has added benefits for the efficiency and security of the geological storage. Moreover, steady state is reached faster by injecting at higher pressures. Higher densities at the bottomhole can also be achieved by a fluctuating injection regime, which also has the advantage of enhancing the CO_2 storage efficiency. Pressure-controlled injection may induce high densities as well, although at a reduced injected mass of CO_2.

It is concluded that CO_2 injection conditions should be tuned considering a balance between optimal storage densities and the stability of the operation. The present model could also be used to determine operating conditions leading to undesired blowout episodes.

6. References

1. Altunin, V.V. and Sakhabetdinov, M.A., Viscosity of liquid and gaseous carbon dioxide at temperatures 220-1300 K and pressure up to 1200 bar, *Teploenergetika*, **8**, 85-89 (1972).
2. Han, W.S., Stillman, G.A., Lu, M., McPherson, B.J., and Park, E., Evaluation of potential nonisothermal processes and heat transport during CO_2 sequestration, *Journal of Geophysical Research*, **115**, B07209, doi:10.1029/2009JB006745 (2010).
3. Hasan, A.R. and Kabir, C.S., *Fluid flow and heat transfer in wellbores*. SPE Richardson, TX, USA (2002).
4. Hidalgo, J. and Carrera, J., Effect of dispersion on the onset of convection during CO_2 sequestration, *Journal of Fluid Mechanics*, **640**, 441-452 (2009).
5. Lu, M. and Connell, L.D., Non-isothermal flow of carbon dioxide in injection wells during geological storage, *International Journal of Greenhouse Gas Control*, **2**, 248-258 (2008).
6. Lu, M. and Connell, L.D., The transient behaviour of CO_2 flow with phase transition in injection wells during geological storage, *Journal of Petroleum Science and Engineering*, **124**, 7-18 (2014).
7. Nimtz, M., Klatt, M., Wiese, B., Kühn, M. and Krautz, H.J., Modelling of the CO_2 process- and transport chain in CCS systems-Examination of transport and storage processes, *Chemie der Erde*, **70**, 185-192 (2010).
8. Pan, L.H., Oldenburg, C.M., and Pruess, K., Transient CO_2 leakage and injection in wellbore-reservoir systems for geological carbon sequestration, *Greenhouse Gases: Science and Technology*, **1(4)**, 335-350 (2011).
9. Pan, L.H., and Oldenburg, C.M., T2Well - An integrated wellbore-reservoir simulator, *Computer and Geosciences*, **65**, 46-55 (2014).
10. Redlich, O. and Kwong, J.N.S., On the thermodynamics of solutions. V. An equation of state. Fugacities of gaseous solutions, *Chemical Reviews* **44(1)**, 233-244 (1949).
11. Sponagle, B., Amadu, M., Groulx, D., and Pegg, M., Modeling of the heat transfer between a CO_2 sequestration well and the surrounding geological formation, Excerpt from the *Proceedings of the 2011 Comsol Conference in Boston*, (2011).
12. Spycher, N., Pruess, K. and Ennis-King, J., CO_2-H_2O Mixtures in the Geological Sequestration of CO_2. I. Assessment and calculation of mutual solubilities from 12 to 100°C and up to 600 bar, *Geochimica et Cosmochimica Acta*, **67**, 3015-3031 (2003).
13. Vilarrasa, V., Silva, O., Carrera, J. and Olivella, S., Liquid CO_2 injection for geological storage in deep saline aquifers, *International Journal of Greenhouse Gas Control*, **14**, 84-96 (2013).
14. Zigrang, D.J. and Sylvester, N.D., A review of explicit friction factor equations, *Journal of Energy Resources Technology* **107(2)**, 280-283 (1985).

7. Acknowledgements

The support received from the MINECO (Torres Quevedo Programme) and the European Social Fund is very much acknowledged.